

Reheating constraints on modified quadratic chaotic inflation

Sudhava Yadav¹, Rajesh Goswami², K.K Venkataratnam^{1,*} and Urjit A. Yajnik^{3,4}

¹ Department of Physics, Malaviya National Institute of Technology Jaipur, Jaipur 302017, India

² Department of Physics, National Institute of Technology Puducherry, Puducherry 609609, India

³ Department of Physics, Indian Institute of Technology Bombay, Mumbai 400076, India

⁴ Department of Physics, Indian Institute of Technology Gandhinagar, Gujarat 382424, India

March 14, 2024

Abstract

The Reheating era of inflationary universe can be parameterized by various parameters like reheating temperature T_{re} , reheating duration N_{re} and average equation of state parameter \bar{w}_{re} , which can be constrained by observationally feasible values of scalar power spectral amplitude A_s and spectral index n_s . In this work, by considering the quadratic chaotic inflationary potential with logarithmic-correction in mass, we examine the reheating era in order to place some limits on model's parameter space. By investigating the reheating epoch using Planck 2018+BK18+BAO data, we show that even a small correction can make the quadratic chaotic model consistent with latest cosmological observations. We also find that the study of reheating era helps to put much tighter constraints on model and effectively improves accuracy of model.

1 Introduction

The inflationary paradigm [1–5] is an exciting and influential epoch of the cosmological universe. It has come up as an aid to resolve a range of well-known cosmological problems like flatness, horizon and monopole problems of famous cosmological big bang theory. The semi-classical theory of inflation generates seeds for Cosmic Microwave Background anisotropy and Large Scale Structures in the late universe [6–8]. Inflation predicts adiabatic, gaussian and almost scale invariant density fluctuations, which are validated by CMB observations like Cosmic Background Explorer (COBE) [9], Wilkinson Microwave Anisotropy Probe (WMAP) [10, 11] and Planck space probe [12–17].

In the realm of inflationary cosmology, a typical scenario involves the presence of a scalar field, which is referred to as the inflaton (ϕ), whose potential energy dominates the universe. In this picture, inflaton slowly rolls through its potential, and the coupling of quantum fluctuations of this scalar field with metric fluctuations is the source of primordial density perturbations called scalar perturbations. The tensor part of the metric has vacuum fluctuations resulting in primordial gravitational waves called tensor perturbations. During inflation, power spectra for both these perturbations depend on a potential called inflaton potential $V(\phi)$.

As Inflation ends, the universe reaches a highly nonthermal and frigid state with no matter content in it. However, the universe must be thermalized at extremely high temperature for big-bang nucleosynthesis (BBN) and baryogenesis. This is attained by ‘reheating’[18–24], transit between the inflationary phase and an era of radiation and matter dominance.

*Corresponding author

There is no established science for reheating era and there is also a lack of direct observational data in favor of reheating. However, recent CMB data helped to obtain indirect bounds for various reheating parameters [25–31], and those parameters are: the reheating temperature (T_{re}), the effective equation of state (EoS) parameter during reheating (ω_{re}) and lastly, the reheating duration, which can be written in the form of number of e-folds (N_{re}). It is challenging to bound the reheating temperature by LSS and CMB observations. However, its value is assumed to be higher than the electroweak scale for dark matter production at a weak scale. A lower limit has been set on reheat temperature i.e. ($T_{\text{re}} \sim 10^{-2} \text{GeV}$) for a successful primordial nucleosynthesis (BBN) [32] and instantaneous reheating consideration allows us to put an upper bound i.e. ($T_{\text{re}} \sim 10^{16} \text{GeV}$) for Planck’s recent upper bound on tensor-to-scalar ratio (r). The value of second parameter, ω_{re} , shifts from $-\frac{1}{3}$ to 1 in various scenarios. It is 0 for reheating generated by perturbative decay of a large inflaton and $\frac{1}{3}$ for instantaneous reheating. The next parameter in line is the duration of reheating phase, N_{re} . Generally, it is incorporated by giving a range of N_k , the number of e-foldings from Hubble crossing of a Fourier mode k to the termination of inflation. N_k has value in the range 46 to 70 in order to work out the horizon problem. These bounds arise by considering reheat temperature at electroweak scale and instantaneous reheating of the universe. A comprehensive analysis of higher bound on N_k is presented in [33, 34].

The relation between inflationary parameters and reheating can be derived by taking into consideration the progression of observable scales of cosmology from the moment of their Hubble crossing during inflation to the current time. We can deduce relations among T_{re} , N_{re} and ω_{re} , the scalar power spectrum amplitude (A_s) and spectral index n_s for single-field inflationary models. Further, the constraints on T_{re} and N_{re} can be obtained from recent CMB data.

Although plenty of inflationary models have been studied in recent years[35] and the inflationary predictions are in agreement with the recent CMB observations, there is still a need for a unique model. The most famous chaotic inflation with quadratic potential ($\frac{1}{2}m^2\phi^2$) is eliminated by recent cosmological observations as it predicts large tensor perturbations due to large potential energy it has during inflaton at large field amplitudes. Hence, lowering the potential at higher field values can help getting rid of this obstacle. Numerous hypotheses in this vein have been put forth [36–45]. Radiative corrections provide an intriguing possibility [36–38] where, generally, the quadratic potential gets flatter as result of running of inflaton’s quartic coupling. This article will rather examine a straightforward scenario in which the mass exhibits a running behaviour described as [46]:

$$m^2(\phi) = m^2 \left(1 - K \ln \left[\frac{\phi^2}{M^2} \right] \right), \quad (1)$$

where M is large mass scale and K is some positive constant. The positive K and the negative sign in above equation is a defining characteristic of dominance of the coupling of inflaton field to fermion fields. The reason for considering the fermionic corrections over bosonic ones is that the earlier ones are likely to flatten the potential, lowering the value of tensor to scalar ratio(r). Hence, making the potential compatible with recent observations[47]. In contrast, the bosonic ones steepen the potential and increase the r value[37, 38, 48]. Another interesting way to make such models compatible with observation is by extension of standard model as done in Ref. [49, 50].

Reheating is well known technique of constraining the inflationary models. There are various ways to analyse the reheating phase as available in literature e.g. one stage reheating study [31, 51], two stage reheating study [52, 53]. In Ref. [54] reheating was analysed through perturbative decay of inflaton to either bosonic or fermionic states through trilinear coupling. Considering one stage reheating technique of constraining the models, we use various reheating parameters to put much tighter bounds on parameter space of quadratic chaotic inflationary model with a logarithmic-correction in mass in light of Planck 2018+BK18+BAO data [16, 17, 47]. By demanding $T_{\text{re}} > 100 \text{ GeV}$ for production of weak-scale dark matter and working in plausible range of average equation of state (EoS) parameter ($-\frac{1}{3} \leq \bar{\omega}_{\text{re}} \leq 1$), we employ the derived relation between inflationary and reheating parameters and observationally feasible values of A_s , n_s and r to place a limit on model’s parameter space. It is a helpful and fairly new tool for putting relatively tighter constraints on the model and reducing its viable parameter space, providing significant improvement in accuracy of the model. Additionally, this technique well differentiate various inflation models as they can have the same forecasts for n_s and r , but definitely not for the same ω_{re} , as the tightened constraints on n_s will result in an increasingly narrow permitted range of ω_{re} for a particular inflationary model.

The organization of this paper is as follows: In Sec. 2 we discuss the dynamics and predictions of slow-roll inflation. We also derived the expressions for T_{re} and N_{re} as a function of $\bar{\omega}_{\text{re}}$ and other inflationary parameters like ΔN_k and V_{end} . In section 3, the Subsec. 3.1 has our recreated data for reheating scenario of simple quadratic chaotic potential. In Subsec. 3.2, we discussed the various field domains within which inflation can occur for quadratic chaotic potential with logarithmic correction in mass and then we parameterized reheating for this model using T_{re} and N_{re} as a function of the scalar spectral index n_s for different ω_{re} . We have also examined the observational limits and reheating parameters for both these models using Planck 2018+BK18+BAO data in Sec. 3. Sec. 4 is reserved for discussion and conclusions.

We will be working with $\hbar = c = 1$ units and the values of some standard parameters used are reduced Planck's mass $M_P = \sqrt{\frac{1}{8\pi G}} = 2.435 \times 10^{18}$ GeV, the redshift of matter radiation equality $z_{\text{eq}} \approx 3400$, $g_{\text{re}} \approx 100$ [27] and the present value of Hubble parameter $H_o = 100h \text{ km s}^{-1} \text{ Mpc}^{-1}$ with $h = 0.68$ [16, 17]

2 Parameterizing reheating in slow-roll inflationary models

Reheating phase can be parameterized by assuming it been dominated by some fluid [55] of energy density ρ with pressure P and equation of state(EoS) parameter $\omega_{\text{re}} = \frac{P}{\rho}$ where

$$\rho = \frac{\dot{\phi}^2}{2} + V(\phi), \quad P = \frac{\dot{\phi}^2}{2} - V(\phi). \quad (2)$$

The continuity equation gives

$$\dot{\rho} + 3H(P + \rho) = 0, \quad (3)$$

$$\dot{\rho} + 3H\rho(\omega_{\text{re}} + 1) = 0. \quad (4)$$

We analyze the dynamics of inflation by considering inflaton ϕ with potential $V(\phi)$ evolving slowly with slow-roll parameters ϵ and η . The approximation of Friedman equation using slow-roll conditions give

$$3H\dot{\phi} + V'(\phi) = 0, \quad (5)$$

$$H^2 = \frac{V(\phi)}{3M_P^2}, \quad (6)$$

where prime (') denotes derivative w.r.t ϕ and $H = \frac{\dot{a}}{a}$ is Hubble parameter. The definition of slow-roll parameter give

$$\epsilon = \frac{M_P^2}{2} \left(\frac{V'}{V} \right)^2, \quad \eta = M_P^2 \left(\frac{V''}{V} \right). \quad (7)$$

The scalar spectral index n_s , tensor spectral index n_T and tensor to scalar ratio r in terms of above slow-roll parameters satisfy the relations

$$n_s = 1 - 6\epsilon + 2\eta, \quad n_T = -2\epsilon, \quad r = 16\epsilon. \quad (8)$$

Now, the number of e-foldings in between Hubble crossing of mode k and termination of inflation denoted by subscript "end" can be given as

$$\Delta N_k = \ln \left(\frac{a_{\text{end}}}{a_k} \right) = \frac{1}{M_P^2} \int_{\phi_{\text{end}}}^{\phi_k} \frac{V}{V'} d\phi, \quad (9)$$

where a_k and ϕ_k represents value of scale factor and inflaton at the point of time when k crosses the Hubble radius. The later part of eq. (9) is obtained using the slow-roll approximations $\ddot{\phi} \ll 3H\dot{\phi}$ and $V(\phi) \gg \dot{\phi}^2$. Similarly,

$$N_{\text{re}} = \ln \left(\frac{a_{\text{re}}}{a_{\text{end}}} \right), \quad (10)$$

Here the quantity N_{re} encrypts both, an era of preheating [22, 56–60] as well as later thermalization process. An energy density controls the Universe’s subsequent evolution and can be written as

$$\rho_{\text{re}} = \frac{\pi^2}{30} g_{\text{re}} T_{\text{re}}^4, \quad (11)$$

where g_{re} gives the actual count of relativistic species at termination of reheating epoch and T_{re} is the reheating temperature. Now, in view of eq. (3)

$$\rho_{\text{re}} = \rho_{\text{end}} e^{-3N_{\text{re}}(1+\bar{\omega}_{\text{re}})}, \quad (12)$$

$$\text{where } \bar{\omega}_{\text{re}} = \langle \omega \rangle = \frac{1}{N_{\text{re}}} \int_{N_{\text{end}}}^N \omega_{\text{re}}(N) dN \quad (13)$$

Here $\bar{\omega}_{\text{re}}$ is average EoS parameter during reheating [25, 51]. Now, eq. (12) can be recast as

$$\frac{a_{\text{re}}}{a_{\text{end}}} = e^{N_{\text{re}}} = \left(\frac{\rho_{\text{re}}}{\rho_{\text{end}}} \right)^{-\frac{1}{3(1+\bar{\omega}_{\text{re}})}}. \quad (14)$$

Using eq. (11) and eq. (14), reheating e-folds N_{re} can be written as

$$N_{\text{re}} = \frac{1}{3(1+\bar{\omega}_{\text{re}})} \left\{ \ln \left(\frac{3}{2} V_{\text{end}} \right) - \ln \left(\frac{\pi^2}{30} g_{\text{re}} \right) \right\} - \frac{4}{3(1+\bar{\omega}_{\text{re}})} \ln(T_{\text{re}}). \quad (15)$$

For some physical scale k , the observed wavenumber ‘ $\frac{k}{a}$ ’ can be given in terms of above known quantities and the redshift during matter-radiation equality epoch (z_{eq}) as [51]

$$H_k = \frac{k}{a_k} = (1+z_{\text{eq}}) \frac{k}{a_o} \rho_{\text{re}}^{\frac{3\bar{\omega}_{\text{re}}-1}{12(1+\bar{\omega}_{\text{re}})}} \rho_{\text{eq}}^{-\frac{1}{4}} \left(\frac{3}{2} V_{\text{end}} \right)^{\frac{1}{3(1+\bar{\omega}_{\text{re}})}} e^{\Delta N_k}. \quad (16)$$

Using eq. (16), ΔN_k can be given as

$$\Delta N_k = \ln H_k - \ln(1+z_{\text{eq}}) - \ln \left(\frac{k}{a_o} \right) - \frac{1}{3(\bar{\omega}_{\text{re}}+1)} \ln \left(\frac{3}{2} V_{\text{end}} \right) - \frac{3\bar{\omega}_{\text{re}}-1}{3(1+\bar{\omega}_{\text{re}})} \ln \left(\rho_{\text{re}}^{\frac{1}{4}} \right) + \ln \left(\rho_{\text{eq}}^{\frac{1}{4}} \right). \quad (17)$$

Inverting eq. (17), and using eq. (11) one can get a mutual relation among the numerous parameters introduced,

$$\ln(T_{\text{re}}) = \frac{3(1+\bar{\omega}_{\text{re}})}{3\bar{\omega}_{\text{re}}-1} \left\{ \ln H_k - \ln(1+z_{\text{eq}}) - \ln \frac{k}{a_o} - \Delta N_k + \ln \left(\rho_{\text{eq}}^{\frac{1}{4}} \right) \right\} - \frac{1}{3\bar{\omega}_{\text{re}}-1} \ln \left(\frac{3}{2} V_{\text{end}} \right) - \frac{1}{4} \ln \left(\frac{\pi^2}{30} g_{\text{re}} \right). \quad (18)$$

The expression for T_{re} from eq. (15) is substituted in eq. (18) to get the expression for N_{re} as mentioned below

$$N_{\text{re}} = \frac{1}{3\bar{\omega}_{\text{re}}-1} \ln \left(\frac{3}{2} V_{\text{end}} \right) + \frac{4}{3\bar{\omega}_{\text{re}}-1} \left\{ \ln \left(\frac{k}{a_o} \right) + \Delta N_k + \ln(1+z_{\text{eq}}) - \ln \left(\rho_{\text{eq}}^{\frac{1}{4}} \right) - \ln H_k \right\} \quad (19)$$

eq. (18) and eq. (19) are the two key relationships for parameterizing reheating in slow-roll inflationary models.

3 Inflationary models

3.1 Quadratic Chaotic inflationary model

We are first considering simple quadratic chaotic potential before moving to its modified form. The quadratic chaotic potential [4] has the form

$$V = \frac{1}{2}m^2\phi^2. \quad (20)$$

The reheating study of this potential was already done in [51] in light of Planck's 2015 data. We are recreating the data by doing the similar study using Planck 2018+BK18+BAO data. Using eq. (7) slow-roll parameters for this potential can be given as

$$\epsilon = \eta = \frac{2M_P^2}{\phi^2}. \quad (21)$$

The Hubble parameter during the crossing of Hubble radius by scale k for this model can be written as

$$H_k^2 = \frac{1}{M_P^2} \left(\frac{V_k}{3 - \epsilon_k} \right) = \frac{1}{2M_P^2} \left(\frac{m^2\phi_k^2}{3 - 2\frac{M_P^2}{\phi_k^2}} \right). \quad (22)$$

where ϕ_k , ϵ_k and V_k respectively represent the inflaton field, slow-roll parameter and potential during crossing of Hubble radius by mode k .

Using the condition $\epsilon = 1$, defining end of inflation, in eq. (21), we obtained $\frac{\phi_{\text{end}}^2}{M_P^2} = 2$

Now, corresponding to pivot scale k_* , used in Planck collaboration, $\frac{k_*}{a_o} = 0.05Mpc^{-1}$, consider the mode k_* crossing the hubble radius at a point where the field has achieved the value ϕ_* during inflation. The remaining number of e-folds persist subsequent to crossing of hubble radius by k_* are

$$\Delta N_* \simeq \frac{1}{M_P^2} \int_{\phi_{\text{end}}}^{\phi_*} \frac{V}{V'} d\phi = \left[\left(\frac{\phi_*}{2M_P} \right)^2 - \frac{1}{2} \right]. \quad (23)$$

The spectral index for this model can be easily obtained using eq. (8) as

$$n_s = 1 - 8 \left(\frac{M_P^2}{\phi_*^2} \right). \quad (24)$$

Now, the formulation for tensor-to-scalar ratio from eq. (8) gives

$$r = 32 \frac{M_P^2}{\phi_*^2}. \quad (25)$$

Moreover, this model yields the relation

$$H_* = \pi M_P \sqrt{16A_s \frac{M_P^2}{\phi_*^2}}. \quad (26)$$

The relation of field ϕ and H eq. (6), and the condition for termination of inflation as used in eq. (23), along with eq. (26) gives expression for V_{end} as

$$V_{\text{end}}(\phi) = \frac{1}{2}m^2\phi_{\text{end}}^2 = \frac{3H_*^2 M_P^2 \phi_{\text{end}}^2}{\phi_*^2} = \frac{6H_*^2 M_P^4}{\phi_*^2}. \quad (27)$$

Now, the expressions for ΔN_* , r , H_* and V_{end} as a function of n_s can be obtained by putting the value of ϕ_* from eq. (24) in eqs. (23), (25), (26) and (27), and then these expressions along with eqs. (18) and (19) gives number of reheating e-folds N_{re} and reheating temperature T_{re} . Planck's 2018 value of $A_s = 2.1 \times 10^{-9}$ and computed value of $\rho_{\text{eq}}^{\frac{1}{4}} = 10^{-9}\text{GeV}$ [16, 17] have been used for calculation. The N_{re} and T_{re} versus n_s plots, along with Planck-2018 1σ bound on n_s i.e. ($0.962 \leq n_s \leq 0.971$) (dark gray) and 2σ bound on n_s i.e. ($0.958 \leq n_s \leq 0.975$) (light gray), for this model are presented graphically in figure 1 for a range of average EoS parameter during reheating.

By demanding $T_{\text{re}} \geq 100$ GeV for production of weak-scale dark matter and solving eqs. (18) and (24), the bounds on n_s are obtained and are reflected on eq. (23) and eq. (25) to obtain bounds on ΔN_* and r . All the

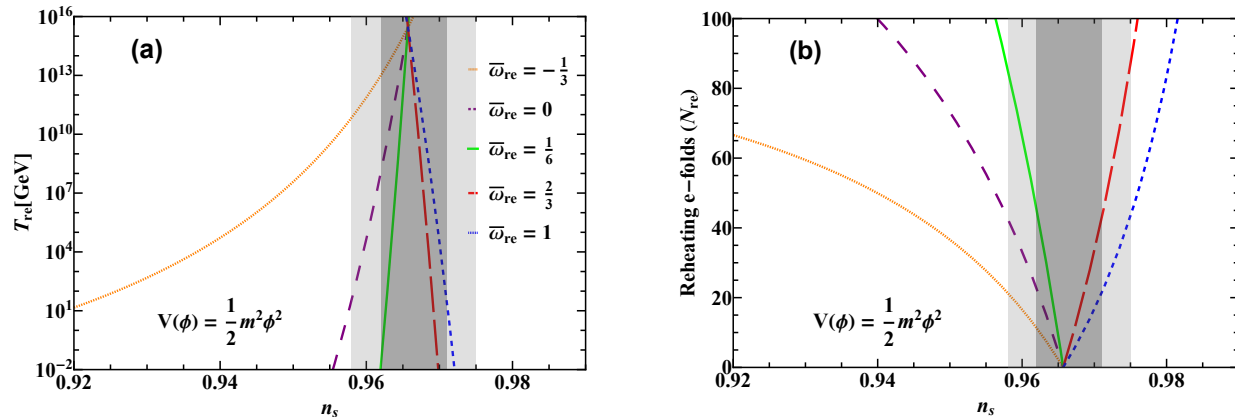


Figure 1: The plots for (a) T_{re} and (b) N_{re} versus n_s for the quadratic chaotic model $V(\phi) = \frac{1}{2}m^2\phi^2$ for different values of \bar{w}_{re} : $\bar{w}_{re} = -\frac{1}{3}$ (dotted orange), $\bar{w}_{re} = 0$ (medium dashed purple), $\bar{w}_{re} = \frac{1}{6}$ (solid green), $\bar{w}_{re} = \frac{2}{3}$ (large dashed red), $\bar{w}_{re} = 1$ (small dashed blue). The regions with light and dark gray shades, respectively, represent the 2σ and 1σ bounds on n_s from Planck 2018 (TE,EE,TT+Low E+Lensing)+BK18+BAO data [16, 17, 47]

obtained bounds are shown in table 1. For this model the bounds on n_s lies inside Planck 2018+BK18+BAO 2σ bound demanding \bar{w}_{re} lies in the range ($0 \leq \bar{w}_{re} \leq 1$) and the corresponding range for r is ($0.169 \geq r \geq 0.117$) while if we demand n_s to lie within 1σ bound then the allowed range of \bar{w}_{re} is ($0.127 \leq \bar{w}_{re} \leq 1$) and the corresponding r values are ($0.152 \geq r \geq 0.117$). Within these ranges of \bar{w}_{re} the tensor-to-scalar ratio (r) is greater than the Planck 2018 and BK18 bound ($r < 0.036$) [47].

From table 1, we can see that all the r values for this model are greater than the combined Planck

Table 1: The permissible range for values of n_s , ΔN_* and r for Quadratic Chaotic inflationary potential ($\frac{1}{2}m^2\phi^2$) by demanding $T_{re} \geq 100 GeV$

	Average Equation of state	n_s	ΔN_*	r
$(\frac{1}{2}m^2\phi^2)$	$-\frac{1}{3} \leq \bar{w}_{re} \leq 0$	$0.926 \leq n_s \leq 0.958$	$26.47 \leq \Delta N_* \leq 47.45$	$0.297 \geq r \geq 0.166$
	$0 \leq \bar{w}_{re} \leq \frac{1}{6}$	$0.958 \leq n_s \leq 0.963$	$47.45 \leq \Delta N_* \leq 53.38$	$0.166 \geq r \geq 0.148$
	$\frac{1}{6} \leq \bar{w}_{re} \leq \frac{2}{3}$	$0.963 \leq n_s \leq 0.969$	$53.38 \leq \Delta N_* \leq 63.99$	$0.148 \geq r \geq 0.124$
	$\frac{2}{3} \leq \bar{w}_{re} \leq 1$	$0.969 \leq n_s \leq 0.971$	$63.99 \leq \Delta N_* \leq 68.10$	$0.124 \geq r \geq 0.117$

2018+BK18+BAO bound ($r < 0.036$) [47]. Hence, this model is incompatible with the data for any choice of \bar{w}_{re} taken.

3.2 Modified quadratic chaotic inflation

The quadratic chaotic inflationary potential with logarithmic-correction in mass term has the form [38, 46]

$$V(\phi) = \frac{1}{2}m^2 \left(1 - K \ln \frac{\phi^2}{M_P^2}\right) \phi^2 = (M')^4 \left(1 - K \ln \frac{\phi^2}{M_P^2}\right) \frac{\phi^2}{M_P^2}, \quad (28)$$

where $(M')^4 = m^2 M_P^2 / 2$ and K is some positive constant. The positive K is a defining characteristic of dominance of fermion couplings. This work is inspired by Ref. [36, 46], where the inflationary scenario of this potential was studied. We are considering this potential in context of reheating in light of Planck 2018+BK18+BAO data.

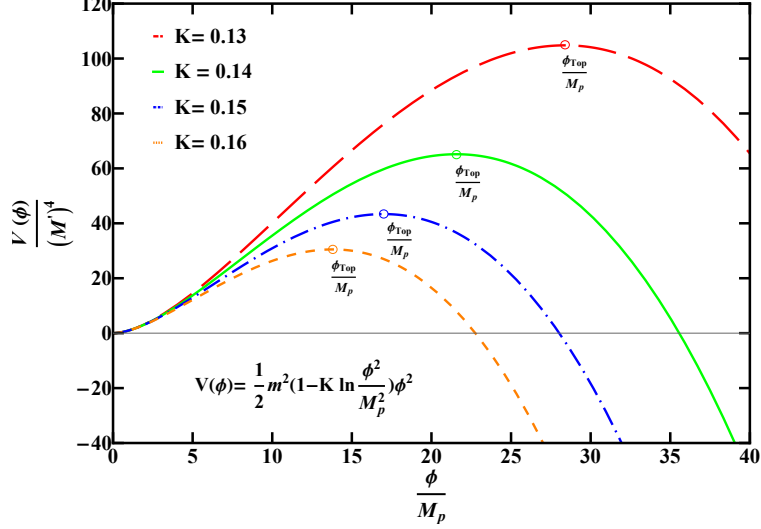


Figure 2: The plot of potential versus $\frac{\phi}{M_P}$ for quadratic chaotic model with corrected mass $V(\phi) = \frac{1}{2}m^2 \left(1 - K \ln \frac{\phi^2}{M_P^2}\right) \phi^2$ for different values of K : $K=0.13$ (large dashed red), $K=0.14$ (solid green), $K=0.15$ (dot-dashed blue), $K=0.16$ (small dashed orange). The small circle on each curve signifies the maxima of potential in each case and the corresponding field value at maxima is $\frac{\phi_{Top}}{M_P}$.

We will start our discussion with various field domains [35] within which inflationary phenomena may occur for above potential. It is evident that the above-mentioned potential eq. (28) does not exhibit positive definiteness for all values of the field (ϕ). The value of this potential becomes negative after a specific point

$$\frac{\phi_{V=0}}{M_P} = \sqrt{e^{\frac{1}{K}}}. \quad (29)$$

The model can only be defined within a specific regime i.e., $\phi < \phi_{V=0}$. On the contrary, the highest point of the potential function, where $V' = 0$ (or can say $\epsilon = 0$), corresponds to field value given as:

$$\frac{\phi_{V'=0}}{M_P} = \frac{\phi_{Top}}{M_P} = \sqrt{e^{\frac{1-K}{K}}}, \quad (30)$$

The model has a sense provided the correction term doesn't have its dominance on the potential, hence the suitable regime is $\phi < \phi_{Top} < \phi_{V=0}$. We have ignored the additional stabilizing terms coming from stability of potential at higher field region as inflation is taking place for field region below the maxima(ϕ_{Top}), which is a stable potential region. Most naturally, inflation begins at an energy density closer to Planck scale and it's observable part takes place at much lower energy density. After the initial inflationary phase if there exist a field region close to maxima, eternal inflation happens and that region will always be dominating. See e.g. refs [36, 61, 62] for more discussion on this point. The potential versus $\frac{\phi}{M_P}$ plot for four different values of K is depicted in figure 2. From figure 2 it can be seen that each K has specific viable regime in which the model is defined and have a sense and we will be working in these regions only.

Now moving further, the slow-roll parameters for this potential can be given as

$$\epsilon = 2M_P^2 \left(\frac{1 - K \left(1 + \ln \frac{\phi^2}{M_P^2}\right)}{\phi \left(1 - K \ln \frac{\phi^2}{M_P^2}\right)} \right)^2, \quad (31)$$

$$\eta = \frac{2M_P^2 \left(-3K + 1 - K \ln \frac{\phi^2}{M_P^2}\right)}{\phi^2 \left(1 - K \ln \frac{\phi^2}{M_P^2}\right)}. \quad (32)$$

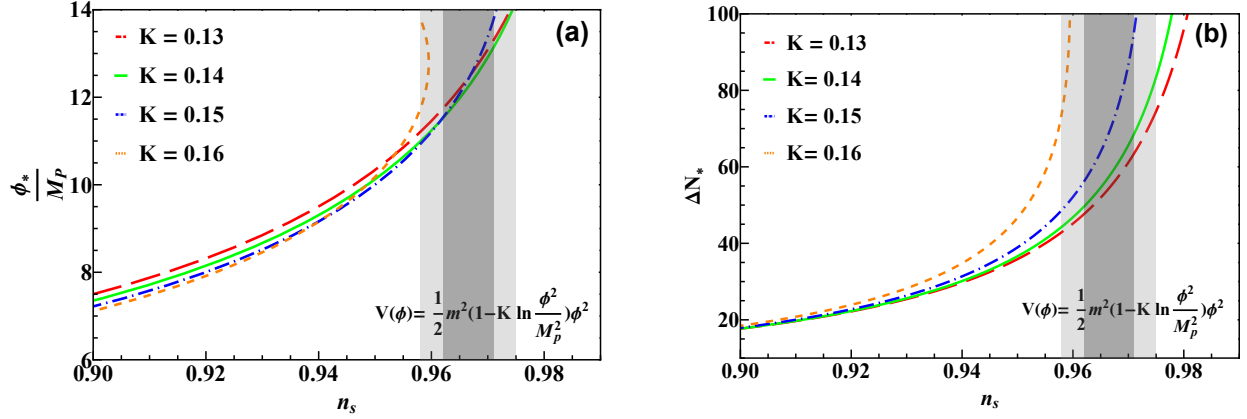


Figure 3: The plots of (a) $\frac{\phi_*}{M_P}$ and (b) ΔN_* versus n_s for quadratic chaotic model with corrected mass $V(\phi) = \frac{1}{2}m^2 \left(1 - K \ln \frac{\phi^2}{M_P^2}\right) \phi^2$ for different values of K . The shaded regions and color codings are same as in figure 1 and 2 respectively.

After substituting the values of ϵ eq. (31) and η eq. (32) in eq. (8), we can write scalar spectral index as

$$n_s = \frac{-4(2 - 3K + 3K^2) + \frac{\phi^2}{M_P^2} - 2K \left(-8 + 6K + \frac{\phi^2}{M_P^2}\right) \ln \frac{\phi^2}{M_P^2} + K^2 \left(-8 + \frac{\phi^2}{M_P^2}\right) \ln \left[\frac{\phi^2}{M_P^2}\right]^2}{\frac{\phi^2}{M_P^2} \left(-1 + K \ln \frac{\phi^2}{M_P^2}\right)^2}. \quad (33)$$

The Hubble parameter during the crossing of Hubble radius by scale k can be written as

$$H_k^2 = \frac{1}{M_P^2} \left(\frac{V_k}{3 - \epsilon_k} \right) = \left(\frac{\frac{1}{2}m^2 \left(1 - K \ln \frac{\phi_k^2}{M_P^2}\right) \frac{\phi_k^2}{M_P^2}}{3 - 2M_P^2 \left(\frac{1 - K \left(1 + \ln \frac{\phi_k^2}{M_P^2}\right)}{\phi \left(1 - K \ln \frac{\phi_k^2}{M_P^2}\right)} \right)^2} \right). \quad (34)$$

Using the condition $\epsilon = 1$ defining end of inflation, we have obtained $\frac{\phi_{\text{end}}}{M_P}$ for different values of K . The remaining number of e-folds persist subsequent to crossing of Hubble radius by k_* till the termination of inflationary epoch can be given as

$$\Delta N_* \simeq \frac{1}{M_P^2} \int_{\phi_{\text{end}}}^{\phi_*} \frac{V}{V'} d\phi_* = \frac{1}{2M_P^2} \int_{\phi_{\text{end}}}^{\phi_*} \frac{\left(1 - K \ln \frac{\phi^2}{M_P^2}\right) \phi}{1 - K \left(1 + \ln \frac{\phi^2}{M_P^2}\right)} d\phi. \quad (35)$$

Defining $\frac{\phi_*}{M_P} = x$. The spectral index n_s eq. (33), at $\phi = \phi_*$ in terms of x will have the form

$$n_s = \frac{-4(2 - 3K + 3K^2) + x^2 - 2K(-8 + 6K + x^2) \ln x^2 + K^2(-8 + x^2) \ln [x^2]^2}{x^2(-1 + K \ln x^2)^2}. \quad (36)$$

The variation of $\frac{\phi_*}{M_P}$ and ΔN_* with n_s using eq. (36) and eq. (35) for 4 different values of K are shown in figure 3a and 3b respectively. Further in this model, we can write the tensor - to - scalar ratio and H_* as

$$r = 32 \left(\frac{1 - K(1 + \ln x^2)}{x(1 - K \ln x^2)} \right)^2. \quad (37)$$

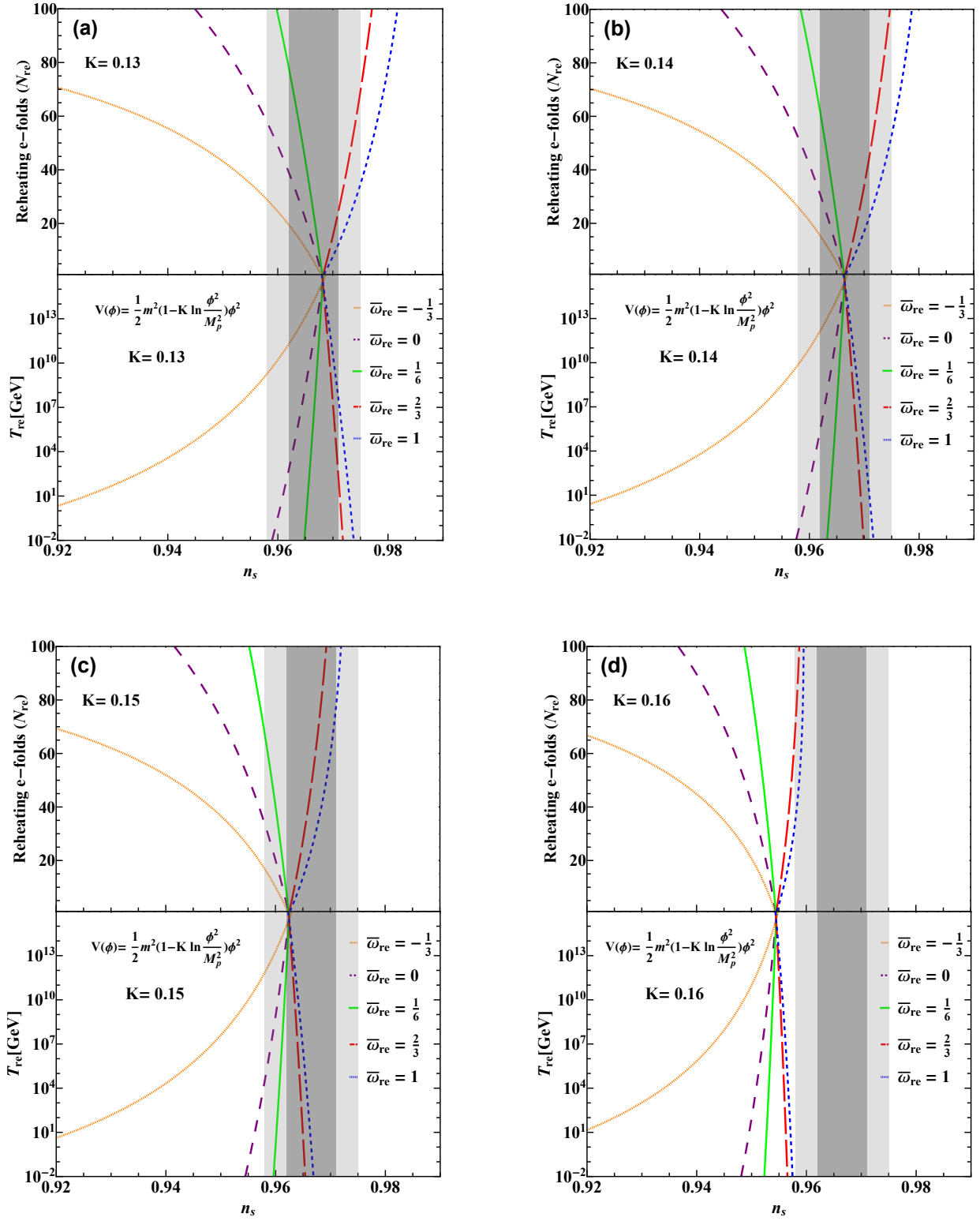


Figure 4: The plots for T_{re} and N_{re} versus spectral index (n_s) for quadratic chaotic model with corrected mass $V(\phi) = \frac{1}{2} m^2 \left(1 - K \ln \frac{\phi^2}{M_p^2}\right) \phi^2$ for different K and $\bar{\omega}_{\text{re}}$ values. The shaded regions and color codings are same as in figure 1

$$H_* = 4\pi M_P \sqrt{A_s} \left(\frac{1 - K(1 + \ln x^2)}{x(1 - K \ln x^2)} \right). \quad (38)$$

Defining $\frac{\phi_{\text{end}}}{M_P} = y$. The relation of field ϕ and H , and the condition for termination of inflation, along with eq. (38) gives expression for V_{end} in terms of x and y as

$$V_{\text{end}}(\phi) = \frac{1}{2} m^2 \left(1 - K \ln \left(\frac{\phi_{\text{end}}^2}{M_P^2} \right) \right) \phi_{\text{end}}^2 = \frac{3H_*^2 M_P^2 (1 - K \ln y^2) y^2}{x^2 (1 - K \ln x^2)}. \quad (39)$$

Now, the value of y obtained using the condition for termination of inflation ($\epsilon = 1$) along with the expressions for ΔN_* , H_* and V_{end} from eqs. (35), (38) and (39) can be inserted in eqs. (18) and (19) and then these two equations along with eq. (36) gives number of reheating e-folds N_{re} and reheating temperature T_{re} . The N_{re} and T_{re} versus n_s plots, along with Planck 2018+BK18+BAO bounds, for 4 different K values for this model are presented graphically in figure 4.

By demanding $T_{\text{re}} > 100$ GeV for production of weak-scale dark matter and solving eqs. (18) and (36), the bounds on n_s are obtained and are reflected on eq. (35) and eq. (37) to obtain bounds on ΔN_* and r . All the obtained bounds for various choices of K are shown in table (2). The r versus n_s plots, along with Planck 2018 (TT,TE,EE+lowE+lensing) and added BK18+BAO constraints, for a range of K values are presented graphically in figure 5. The figure 5 shows that the tensor- to scalar ratio is inside the viable range ($r < 0.036$) for K values closer to $K = 0.15$. The value $K = 0$ gives us the normal quadratic chaotic potential. The range of \bar{w}_{re} for which our obtained data for $K = 0.15$ is compatible with Planck 2018+BK18+BAO 2σ bound on n_s and r give ($0.7 < \bar{w}_{\text{re}} \leq 1$).

We have also found the viable range of the reheat temperature and number of e-foldings for each case which shows compatibility with Planck 2018+BK18+BAO 1σ bound on n_s using figure 4 and the findings have been clearly presented in a tabular format in table 3. The table 3 shows that the curve corresponding to $\bar{w}_{\text{re}} = \frac{1}{6}$ for $K=0.13$, ($\frac{1}{6} \leq \bar{w}_{\text{re}} \leq \frac{2}{3}$) for 0.14 and ($\frac{2}{3} \leq \bar{w}_{\text{re}} \leq 1$) for $K=0.15$, give every possible value of reheating temperature (10^{-2} GeV to 10^{16} GeV) while $K=0.16$ shows incompatibility with data for all \bar{w}_{re} taken. The n_s values for these \bar{w}_{re} ranges are 0.966 for $K=0.13$ and ($0.964 < n_s \leq 0.969$) for 0.14 while it is ($0.965 < n_s \leq 0.966$) for $K=0.15$ which sets limit on tensor to scalar ratio(r) and the obtained values of r are 0.083 for $K=0.13$ and ($0.068 \geq r \geq 0.052$) for 0.14 while it is ($0.037 \geq r \geq 0.033$) for $K=0.15$ and only the r values for $K=0.15$ are satisfying the condition ($r < 0.036$).

4 Discussion and conclusion

In this work, we have considered a modified form of quadratic chaotic inflation. Our primary goal is to study the reheating phase in light of Planck 2018+BK18+BAO observations. For that, we have considered two parameters, namely duration of reheating N_{re} and reheating temperature T_{re} and obtained their variation as function of scalar spectral index n_s by considering a suitable range of effective equation of state \bar{w}_{re} . By demanding $T_{\text{re}} > 100$ GeV for production of weak-scale dark matter and allowing \bar{w}_{re} to vary in the range ($-\frac{1}{3} \leq \bar{w}_{\text{re}} \leq 1$), we tried to find the permissible ranges for n_s , ΔN_* and tensor-to-scalar ratio(r) for our models.

We first restudied the simple quadratic chaotic inflation using the most recent Planck 2018+BK18+BAO data and found that the condition $T_{\text{re}} > 100$ GeV gives ($0 \leq \bar{w}_{\text{re}} \leq 1$) for n_s to lie inside 2σ bounds while if we demand n_s to lie within 1σ bounds than the allowed range of \bar{w}_{re} is ($0.127 \leq \bar{w}_{\text{re}} \leq 1$). Within these ranges of \bar{w}_{re} , r is greater than the observational bound on r , i.e. ($r < 0.036$).

Since the normal quadratic chaotic potential is not favoring the observational data. We have considered a modified form of quadratic chaotic potential where a logarithmic correction containing a model parameter K is added to the mass term. We have found that for each value of model parameter K of the modified model, there is only a specific range of inflaton field (ϕ) within which the model is defined and the correction part is not dominant over the actual quadratic term of potential. We have constrained ourself to only those regions for our analysis. By imposing the reheating conditions on this model, we found that the constraints on n_s and r are consistent with Planck's 2018 and BK18 data for K values closer to ($K = 0.15$). The range of \bar{w}_{re} for which our obtained data is compatible with Planck 2018+BK18+BAO 2σ bound on n_s and r give

Table 2: The permissible range for n_s , ΔN_* and r for different K values for modified Quadratic Chaotic inflation by demanding $T_{re} \geq 100 GeV$

	Average Equation of state	n_s	ΔN_*	r
K = 0.13	$-\frac{1}{3} \leq \bar{\omega}_{re} \leq 0$	$0.932 \leq n_s \leq 0.962$	$26.07 \leq \Delta N_* \leq 47.03$	$0.195 \geq r \geq 0.096$
	$0 \leq \bar{\omega}_{re} \leq \frac{1}{6}$	$0.962 \leq n_s \leq 0.966$	$47.03 \leq \Delta N_* \leq 52.95$	$0.096 \geq r \geq 0.083$
	$\frac{1}{6} \leq \bar{\omega}_{re} \leq \frac{2}{3}$	$0.966 \leq n_s \leq 0.971$	$52.95 \leq \Delta N_* \leq 63.56$	$0.083 \geq r \geq 0.066$
	$\frac{2}{3} \leq \bar{\omega}_{re} \leq 1$	$0.971 \leq n_s \leq 0.973$	$63.56 \leq \Delta N_* \leq 67.68$	$0.066 \geq r \geq 0.060$
K = 0.14	$-\frac{1}{3} \leq \bar{\omega}_{re} \leq 0$	$0.931 \leq n_s \leq 0.960$	$26.02 \leq \Delta N_* \leq 46.94$	$0.175 \geq r \geq 0.080$
	$0 \leq \bar{\omega}_{re} \leq \frac{1}{6}$	$0.960 \leq n_s \leq 0.964$	$46.94 \leq \Delta N_* \leq 52.86$	$0.080 \geq r \geq 0.068$
	$\frac{1}{6} \leq \bar{\omega}_{re} \leq \frac{2}{3}$	$0.964 \leq n_s \leq 0.969$	$52.86 \leq \Delta N_* \leq 63.46$	$0.068 \geq r \geq 0.052$
	$\frac{2}{3} \leq \bar{\omega}_{re} \leq 1$	$0.969 \leq n_s \leq 0.971$	$63.46 \leq \Delta N_* \leq 67.56$	$0.052 \geq r \geq 0.047$
K = 0.15	$-\frac{1}{3} \leq \bar{\omega}_{re} \leq 0$	$0.929 \leq n_s \leq 0.957$	$25.95 \leq \Delta N_* \leq 46.84$	$0.152 \geq r \geq 0.063$
	$0 \leq \bar{\omega}_{re} \leq \frac{1}{6}$	$0.957 \leq n_s \leq 0.960$	$46.84 \leq \Delta N_* \leq 52.74$	$0.063 \geq r \geq 0.052$
	$\frac{1}{6} \leq \bar{\omega}_{re} \leq \frac{2}{3}$	$0.960 \leq n_s \leq 0.965$	$52.74 \leq \Delta N_* \leq 63.31$	$0.052 \geq r \geq 0.037$
	$\frac{2}{3} \leq \bar{\omega}_{re} \leq 1$	$0.965 \leq n_s \leq 0.966$	$63.31 \leq \Delta N_* \leq 67.40$	$0.037 \geq r \geq 0.033$
K = 0.16	$-\frac{1}{3} \leq \bar{\omega}_{re} \leq 0$	$0.925 \leq n_s \leq 0.950$	$25.88 \leq \Delta N_* \leq 46.71$	$0.129 \geq r \geq 0.044$
	$0 \leq \bar{\omega}_{re} \leq \frac{1}{6}$	$0.950 \leq n_s \leq 0.953$	$46.71 \leq \Delta N_* \leq 52.60$	$0.044 \geq r \geq 0.034$
	$\frac{1}{6} \leq \bar{\omega}_{re} \leq \frac{2}{3}$	$0.953 \leq n_s \leq 0.956$	$52.60 \leq \Delta N_* \leq 63.11$	$0.034 \geq r \geq 0.022$
	$\frac{2}{3} \leq \bar{\omega}_{re} \leq 1$	$0.956 \leq n_s \leq 0.957$	$63.11 \leq \Delta N_* \leq 67.18$	$0.022 \geq r \geq 0.019$

Table 3: The range of T_{re} and N_{re} for potential $V(\phi) = \frac{1}{2}m^2 \left(1 - K \ln \frac{\phi^2}{M_P^2}\right) \phi^2$ which shows compatibility with Planck 2018+BK18+BAO

1 σ bound on n_s .

	K = 0.13		K = 0.14		K = 0.15	
	$T_{re}(\text{GeV})$	N_{re}	$T_{re}(\text{GeV})$	N_{re}	$T_{re}(\text{GeV})$	N_{re}
$\bar{\omega}_{re} = -\frac{1}{3}$	$T_{re} \geq 1.95 \times 10^{11}$	$N_{re} \leq 19.53$	$T_{re} \geq 1.50 \times 10^{12}$	$N_{re} \leq 15.40$	$T_{re} \geq 1.12 \times 10^{15}$	$N_{re} \leq 1.62$
$\bar{\omega}_{re} = 0$	$T_{re} \geq 642.01$	$N_{re} \leq 39.07$	$T_{re} \geq 3.07 \times 10^5$	$N_{re} \leq 30.81$	$T_{re} \geq 2.22 \times 10^{14}$	$N_{re} \leq 3.24$
$\bar{\omega}_{re} = \frac{1}{6}$	$10^{16} \geq T_{re} \geq 10^{-2}$	$N_{re} \leq 78.13$	$10^{16} \geq T_{re} \geq 10^{-2}$	$N_{re} \leq 61.61$	$T_{re} \geq 8.7 \times 10^{12}$	$N_{re} \leq 6.48$
$\bar{\omega}_{re} = \frac{2}{3}$	$T_{re} \geq 211.89$	$N_{re} \leq 24.22$	$10^{16} \geq T_{re} \geq 10^{-2}$	$N_{re} \leq 45.13$	$10^{16} \geq T_{re} \geq 10^{-2}$	$N_{re} \geq 0$
$\bar{\omega}_{re} = 1$	$T_{re} \geq 3.85 \times 10^7$	$N_{re} \leq 12.11$	$T_{re} \geq 5.70$	$N_{re} \leq 22.56$	$10^{16} \geq T_{re} \geq 10^{-2}$	$N_{re} \leq 76.75$

($0.7 < \bar{\omega}_{re} \leq 1$) for K=0.15.

Also, from the plots showing the variation of T_{re} with n_s , we have found that different values of K and $\bar{\omega}_{re}$ give different ranges of reheating temperature as compatible with Planck's 1 σ bounds on n_s , but if we allow T_{re} to vary over the whole range (10^{-2} GeV to 10^{16} GeV), then $\bar{\omega}_{re}$ is restricted to ($0.074 \leq \bar{\omega}_{re} \leq 0.570$)

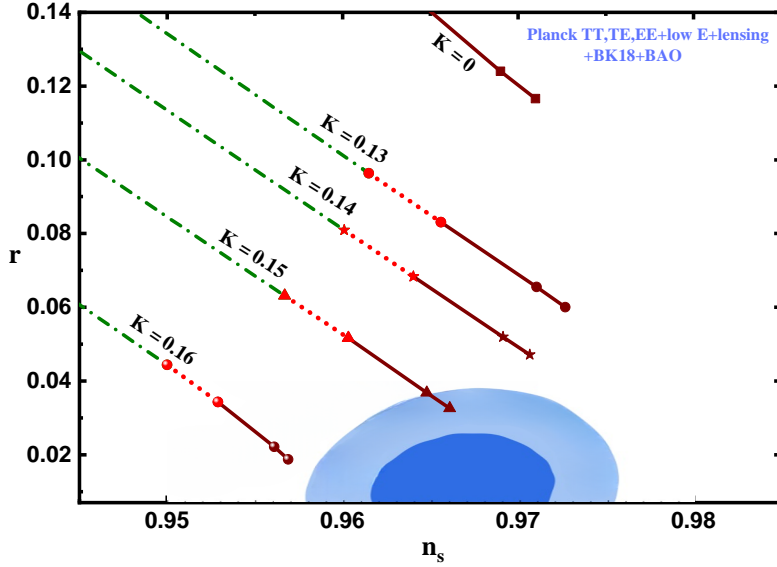


Figure 5: The r versus n_s plots for different values of K over a range of $\bar{\omega}_{re}$ taken: $\bar{\omega}_{re} < 0$ (green), $0 \leq \bar{\omega}_{re} \leq \frac{1}{6}$ (red), $\frac{1}{6} < \bar{\omega}_{re} \leq 1$ (brown). The dark and light blue shadings corresponds to 1σ and 2σ bounds from Planck 2018(TT,TE,EE+lowE+lensing)+BK18+BAO[47].

for $K=0.13$, ($0.120 \leq \bar{\omega}_{re} \leq 0.854$) for $K=0.14$ and ($0.307 \leq \bar{\omega}_{re} \leq 1$) for $K=0.15$ while $K=0.16$ shows incompatibility with 1σ bounds on n_s for all $\bar{\omega}_{re}$ taken.

To conclude, the reheating study shows that the values of K close to 0.15 are the favorable ones and the $\bar{\omega}_{re}$ range satisfying the observational data for $K=0.15$ suggests the possible production of Feebly Interacting Massive Particle(FIMP) and Weakly Interacting Massive Particle(WIMP)-like dark matter particles[63–65] and primordial black holes [66]. Elaborated study of possible particle production will be done in our future publications. The findings of the reheating study prove that even a small correction in mass term can help quadratic chaotic potential to favour the latest cosmological observations. Also, we have found that considering the reheating constraints, the average equation of state parameter $\bar{\omega}_{re}$ plays a vital role in defining the compatible range of reheating parameters, which effectively narrows the model’s viable parameter space and significantly increases the model’s accuracy

Acknowledgments

SY would like to acknowledge the Ministry of Education, Government of India, for providing fellowship. UAY acknowledges support from an Institute Chair Professorship of IIT Bombay.

References

- [1] A. H. Guth, “Inflationary universe: A possible solution to the horizon and flatness problems,” *Physical Review D*, vol. 23, no. 2, pp. 347–356, Jan. 1981. DOI: 10.1103/PhysRevD.23.347.
- [2] A. Starobinsky, “A new type of isotropic cosmological models without singularity,” en, *Physics Letters B*, vol. 91, no. 1, pp. 99–102, Mar. 1980, ISSN: 03702693. DOI: 10.1016/0370-2693(80)90670-X.

- [3] A. Linde, “A new inflationary universe scenario: A possible solution of the horizon, flatness, homogeneity, isotropy and primordial monopole problems,” en, *Physics Letters B*, vol. 108, no. 6, pp. 389–393, Feb. 1982, ISSN: 03702693. DOI: 10.1016/0370-2693(82)91219-9.
- [4] A. Linde, “Chaotic inflation,” en, *Physics Letters B*, vol. 129, no. 3-4, pp. 177–181, Sep. 1983, ISSN: 03702693. DOI: 10.1016/0370-2693(83)90837-7.
- [5] A. Riotto, “Inflation and the Theory of Cosmological Perturbations,” 2002. DOI: 10.48550/ARXIV.HEP-PH/0210162.
- [6] V. F. Mukhanov and G. V. Chibisov, “Quantum fluctuations and a nonsingular universe,” *ZhETF Pisma Redaktsiiu*, vol. 33, pp. 549–553, May 1981, ADS Bibcode: 1981ZhPmR..33..549M.
- [7] A. Starobinsky, “Dynamics of phase transition in the new inflationary universe scenario and generation of perturbations,” en, *Physics Letters B*, vol. 117, no. 3-4, pp. 175–178, Nov. 1982, ISSN: 03702693. DOI: 10.1016/0370-2693(82)90541-X.
- [8] A. H. Guth and S.-Y. Pi, “Quantum mechanics of the scalar field in the new inflationary universe,” en, *Physical Review D*, vol. 32, no. 8, pp. 1899–1920, Oct. 1985, ISSN: 0556-2821. DOI: 10.1103/PhysRevD.32.1899.
- [9] G. F. Smoot *et al.*, “Structure in the COBE Differential Microwave Radiometer First-Year Maps,” *The Astrophysical Journal*, vol. 396, p. L1, Sep. 1992, ADS Bibcode: 1992ApJ...396L...1S, ISSN: 0004-637X. DOI: 10.1086/186504.
- [10] J. Dunkley *et al.*, “FIVE-YEAR WILKINSON MICROWAVE ANISOTROPY PROBE OBSERVATIONS: LIKELIHOODS AND PARAMETERS FROM THE WMAP DATA,” *The Astrophysical Journal Supplement Series*, vol. 180, no. 2, pp. 306–329, Feb. 2009, ISSN: 0067-0049, 1538-4365. DOI: 10.1088/0067-0049/180/2/306.
- [11] E. Komatsu *et al.*, “SEVEN-YEAR WILKINSON MICROWAVE ANISOTROPY PROBE (WMAP) OBSERVATIONS: COSMOLOGICAL INTERPRETATION,” *The Astrophysical Journal Supplement Series*, vol. 192, no. 2, p. 18, Feb. 2011, ISSN: 0067-0049, 1538-4365. DOI: 10.1088/0067-0049/192/2/18.
- [12] P. A. R. Ade *et al.*, “Planck 2013 results. XVI. Cosmological parameters,” *Astronomy & Astrophysics*, vol. 571, A16, Nov. 2014, ISSN: 0004-6361, 1432-0746. DOI: 10.1051/0004-6361/201321591.
- [13] P. A. R. Ade *et al.*, “Planck 2013 results. XXII. Constraints on inflation,” *Astronomy & Astrophysics*, vol. 571, A22, Nov. 2014, ISSN: 0004-6361, 1432-0746. DOI: 10.1051/0004-6361/201321569.
- [14] P. A. R. Ade *et al.*, “Planck 2015 results: XIII. Cosmological parameters,” *Astronomy & Astrophysics*, vol. 594, A13, Oct. 2016, ISSN: 0004-6361, 1432-0746. DOI: 10.1051/0004-6361/201525830.
- [15] P. A. R. Ade *et al.*, “Planck 2015 results: XX. Constraints on inflation,” *Astronomy & Astrophysics*, vol. 594, A20, Oct. 2016, ISSN: 0004-6361, 1432-0746. DOI: 10.1051/0004-6361/201525898.
- [16] N. Aghanim *et al.*, “Planck 2018 results: VI. Cosmological parameters,” *Astronomy & Astrophysics*, vol. 641, A6, Sep. 2020, ISSN: 0004-6361, 1432-0746. DOI: 10.1051/0004-6361/201833910.
- [17] Y. Akrami *et al.*, “Planck 2018 results: X. Constraints on inflation,” *Astronomy & Astrophysics*, vol. 641, A10, Sep. 2020, ISSN: 0004-6361, 1432-0746. DOI: 10.1051/0004-6361/201833887.
- [18] M. S. Turner, “Coherent scalar-field oscillations in an expanding universe,” en, *Physical Review D*, vol. 28, no. 6, pp. 1243–1247, Sep. 1983, ISSN: 0556-2821. DOI: 10.1103/PhysRevD.28.1243.
- [19] J. H. Traschen and R. H. Brandenberger, “Particle production during out-of-equilibrium phase transitions,” en, *Physical Review D*, vol. 42, no. 8, pp. 2491–2504, Oct. 1990, ISSN: 0556-2821. DOI: 10.1103/PhysRevD.42.2491.
- [20] A. Albrecht, P. J. Steinhardt, M. S. Turner, and F. Wilczek, “Reheating an Inflationary Universe,” en, *Physical Review Letters*, vol. 48, no. 20, pp. 1437–1440, May 1982, ISSN: 0031-9007. DOI: 10.1103/PhysRevLett.48.1437.
- [21] L. Kofman, A. Linde, and A. A. Starobinsky, “Reheating after Inflation,” en, *Physical Review Letters*, vol. 73, no. 24, pp. 3195–3198, Dec. 1994, ISSN: 0031-9007. DOI: 10.1103/PhysRevLett.73.3195.

- [22] L. Kofman, A. Linde, and A. A. Starobinsky, “Towards the theory of reheating after inflation,” en, *Physical Review D*, vol. 56, no. 6, pp. 3258–3295, Sep. 1997, ISSN: 0556-2821, 1089-4918. DOI: 10.1103/PhysRevD.56.3258.
- [23] M. Drewes and J. U. Kang, “The kinematics of cosmic reheating,” en, *Nuclear Physics B*, vol. 875, no. 2, pp. 315–350, Oct. 2013, ISSN: 05503213. DOI: 10.1016/j.nuclphysb.2013.07.009.
- [24] R. Allahverdi, R. Brandenberger, F.-Y. Cyr-Racine, and A. Mazumdar, “Reheating in Inflationary Cosmology: Theory and Applications,” en, *Annual Review of Nuclear and Particle Science*, vol. 60, no. 1, pp. 27–51, Nov. 2010, ISSN: 0163-8998, 1545-4134. DOI: 10.1146/annurev.nucl.012809.104511.
- [25] J. Martin, C. Ringeval, and V. Vennin, “Observing Inflationary Reheating,” en, *Physical Review Letters*, vol. 114, no. 8, p. 081303, Feb. 2015, ISSN: 0031-9007, 1079-7114. DOI: 10.1103/PhysRevLett.114.081303.
- [26] J. Martin and C. Ringeval, “First CMB constraints on the inflationary reheating temperature,” en, *Physical Review D*, vol. 82, no. 2, p. 023511, Jul. 2010, ISSN: 1550-7998, 1550-2368. DOI: 10.1103/PhysRevD.82.023511.
- [27] L. Dai, M. Kamionkowski, and J. Wang, “Reheating Constraints to Inflationary Models,” en, *Physical Review Letters*, vol. 113, no. 4, p. 041302, Jul. 2014, ISSN: 0031-9007, 1079-7114. DOI: 10.1103/PhysRevLett.113.041302.
- [28] J. Martin and C. Ringeval, “Inflation after WMAP3: Confronting the slow-roll and exact power spectra with CMB data,” *Journal of Cosmology and Astroparticle Physics*, vol. 2006, no. 08, pp. 009–009, Aug. 2006, ISSN: 1475-7516. DOI: 10.1088/1475-7516/2006/08/009.
- [29] P. Adshead, R. Easther, J. Pritchard, and A. Loeb, “Inflation and the scale dependent spectral index: Prospects and strategies,” *Journal of Cosmology and Astroparticle Physics*, vol. 2011, no. 02, pp. 021–021, Feb. 2011, ISSN: 1475-7516. DOI: 10.1088/1475-7516/2011/02/021.
- [30] J. Mielczarek, “Reheating temperature from the CMB,” en, *Physical Review D*, vol. 83, no. 2, p. 023502, Jan. 2011, ISSN: 1550-7998, 1550-2368. DOI: 10.1103/PhysRevD.83.023502.
- [31] J. L. Cook, E. Dimastrogiovanni, D. A. Easson, and L. M. Krauss, “Reheating predictions in single field inflation,” *Journal of Cosmology and Astroparticle Physics*, vol. 2015, no. 04, pp. 047–047, Apr. 2015, ISSN: 1475-7516. DOI: 10.1088/1475-7516/2015/04/047.
- [32] G. Steigman, “Primordial Nucleosynthesis in the Precision Cosmology Era,” en, *Annual Review of Nuclear and Particle Science*, vol. 57, no. 1, pp. 463–491, Nov. 2007, ISSN: 0163-8998, 1545-4134. DOI: 10.1146/annurev.nucl.56.080805.140437.
- [33] S. Dodelson and L. Hui, “Horizon ratio bound for inflationary fluctuations,” *Physical Review Letters*, vol. 91, no. 13, Sep. 2003. DOI: 10.1103/physrevlett.91.131301.
- [34] A. R. Liddle and S. M. Leach, “How long before the end of inflation were observable perturbations produced?” *Physical Review D*, vol. 68, no. 10, Nov. 2003. DOI: 10.1103/physrevd.68.103503.
- [35] J. Martin, C. Ringeval, and V. Vennin, *Encyclopaedia Inflationaris*, arXiv:1303.3787 [astro-ph, physics:gr-qc, physics:hep-ph, physics:hep-th], Sep. 2013. DOI: 10.48550/arXiv.1303.3787.
- [36] V. N. Şenoğuz and Q. Shafi, “Chaotic inflation, radiative corrections and precision cosmology,” en, *Physics Letters B*, vol. 668, no. 1, pp. 6–10, Sep. 2008, ISSN: 03702693. DOI: 10.1016/j.physletb.2008.08.017.
- [37] K. Enqvist and M. Karčiauskas, “Does Planck really rule out monomial inflation?” *Journal of Cosmology and Astroparticle Physics*, vol. 2014, no. 02, pp. 034–034, Feb. 2014, ISSN: 1475-7516. DOI: 10.1088/1475-7516/2014/02/034.
- [38] G. Ballesteros and C. Tamarit, “Radiative plateau inflation,” en, *Journal of High Energy Physics*, vol. 2016, no. 2, p. 153, Feb. 2016, ISSN: 1029-8479. DOI: 10.1007/JHEP02(2016)153.
- [39] K. Nakayama, F. Takahashi, and T. T. Yanagida, “Polynomial chaotic inflation in the Planck era,” en, *Physics Letters B*, vol. 725, no. 1-3, pp. 111–114, Aug. 2013, ISSN: 03702693. DOI: 10.1016/j.physletb.2013.06.050.

- [40] K. Nakayama and F. Takahashi, “Running kinetic inflation,” *Journal of Cosmology and Astroparticle Physics*, vol. 2010, no. 11, pp. 009–009, Nov. 2010, ISSN: 1475-7516. DOI: 10.1088/1475-7516/2010/11/009.
- [41] C. Pallis, “Kinetically modified nonminimal chaotic inflation,” en, *Physical Review D*, vol. 91, no. 12, p. 123508, Jun. 2015, ISSN: 1550-7998, 1550-2368. DOI: 10.1103/PhysRevD.91.123508.
- [42] K. Kannike *et al.*, “Dynamically induced Planck scale and inflation,” en, *Journal of High Energy Physics*, vol. 2015, no. 5, p. 65, May 2015, ISSN: 1029-8479. DOI: 10.1007/JHEP05(2015)065.
- [43] L. Boubekeur, E. Giusarma, O. Mena, and H. Ramírez, “Do current data prefer a nonminimally coupled inflaton?” en, *Physical Review D*, vol. 91, no. 10, p. 103004, May 2015, ISSN: 1550-7998, 1550-2368. DOI: 10.1103/PhysRevD.91.103004.
- [44] L. Marzola and A. Racioppi, “Minimal but non-minimal inflation and electroweak symmetry breaking,” *Journal of Cosmology and Astroparticle Physics*, vol. 2016, no. 10, pp. 010–010, Oct. 2016, ISSN: 1475-7516. DOI: 10.1088/1475-7516/2016/10/010.
- [45] A. Racioppi, “New universal attractor in nonminimally coupled gravity: Linear inflation,” en, *Physical Review D*, vol. 97, no. 12, p. 123514, Jun. 2018, ISSN: 2470-0010, 2470-0029. DOI: 10.1103/PhysRevD.97.123514.
- [46] S. Kasuya and M. Taira, “Quadratic chaotic inflation with a logarithmic-corrected mass,” en, *Physical Review D*, vol. 98, no. 12, p. 123515, Dec. 2018, ISSN: 2470-0010, 2470-0029. DOI: 10.1103/PhysRevD.98.123515.
- [47] P. A. Ade *et al.*, “Improved constraints on primordial gravitational waves using planck, wmap, and bicep/keck observations through the 2018 observing season,” *Physical review letters*, vol. 127, no. 15, p. 151301, 2021.
- [48] W. Ahmed, O. Ishaque, and M. U. Rehman, “Quantum smearing in hybrid inflation with chaotic potentials,” *International Journal of Modern Physics D*, vol. 25, no. 03, p. 1650035, 2016.
- [49] D. Borah, D. Nanda, and A. K. Saha, “Common origin of modified chaotic inflation, nonthermal dark matter, and Dirac neutrino mass,” *Phys. Rev. D*, vol. 101, no. 7, p. 075006, 2020. DOI: 10.1103/PhysRevD.101.075006. arXiv: 1904.04840 [hep-ph].
- [50] A. Ghoshal, N. Okada, and A. Paul, “eV Hubble scale inflation with a radiative plateau: Very light inflaton, reheating, and dark matter in B-L extensions,” *Phys. Rev. D*, vol. 106, no. 9, p. 095021, 2022. DOI: 10.1103/PhysRevD.106.095021. arXiv: 2203.03670 [hep-ph].
- [51] R. Goswami and U. A. Yajnik, “Reconciling low multipole anomalies and reheating in single field inflationary models,” *Journal of Cosmology and Astroparticle Physics*, vol. 2018, no. 10, pp. 018–018, Oct. 2018, ISSN: 1475-7516. DOI: 10.1088/1475-7516/2018/10/018.
- [52] R. Goswami and U. A. Yajnik, “Reheating constraints to modulus mass for single field inflationary models,” en, *Nuclear Physics B*, vol. 960, p. 115211, Nov. 2020, ISSN: 05503213. DOI: 10.1016/j.nuclphysb.2020.115211.
- [53] D. Maity and P. Saha, “Minimal plateau inflationary cosmologies and constraints from reheating,” *Class. Quant. Grav.*, vol. 36, p. 045010, 2019. DOI: 10.1088/1361-6382/ab0038. arXiv: 1902.01895 [gr-qc].
- [54] M. Drees and Y. Xu, “Small field polynomial inflation: reheating, radiative stability and lower bound,” *JCAP*, vol. 09, p. 012, 2021. DOI: 10.1088/1475-7516/2021/09/012. arXiv: 2104.03977 [hep-ph].
- [55] J. Martin, “Inflation and Precision Cosmology,” 2003. DOI: 10.48550/ARXIV.ASTRO-PH/0312492.
- [56] D. Boyanovsky, H. J. de Vega, R. Holman, and J. F. J. Salgado, “Preheating and Reheating in Inflationary Cosmology: A pedagogical survey,” 1996. DOI: 10.48550/ARXIV.ASTRO-PH/9609007.
- [57] L. Kofman, “Reheating and Preheating after Inflation,” 1998. DOI: 10.48550/ARXIV.HEP-PH/9802285.
- [58] G. Felder, L. Kofman, and A. Linde, “Instant Preheating,” 1998. DOI: 10.48550/ARXIV.HEP-PH/9812289.

- [59] G. F. Giudice, I. I. Tkachev, and A. Riotto, “The cosmological moduli problem and preheating,” *Journal of High Energy Physics*, vol. 2001, no. 06, pp. 020–020, Jun. 2001, ISSN: 1029-8479. DOI: 10.1088/1126-6708/2001/06/020.
- [60] M. Desroche, G. N. Felder, J. M. Kratochvil, and A. Linde, “Preheating in new inflation,” en, *Physical Review D*, vol. 71, no. 10, p. 103516, May 2005, ISSN: 1550-7998, 1550-2368. DOI: 10.1103/PhysRevD.71.103516.
- [61] A. Linde, “Particle physics and inflationary cosmology,” *arXiv preprint hep-th/0503203*, 2005.
- [62] A. Vilenkin, “Birth of inflationary universes,” *Physical Review D*, vol. 27, no. 12, p. 2848, 1983.
- [63] M. R. Haque, D. Maity, and R. Mondal, “Wimps, fimps, and inflaton phenomenology via reheating, cmb and ΔN_{eff} ,” *Journal of High Energy Physics*, vol. 2023, no. 9, p. 12, Sep. 2023. DOI: 10.1007/JHEP09(2023)012.
- [64] M. R. Haque and D. Maity, “Gravitational dark matter: Free streaming and phase space distribution,” *Physical Review D*, vol. 106, no. 2, 023506, p. 023506, Jul. 2022. DOI: 10.1103/PhysRevD.106.023506.
- [65] A. Chakraborty, M. R. Haque, D. Maity, and R. Mondal, “Inflaton phenomenology via reheating in the light of pgws and latest bicep/Keck data,” *arXiv preprint arXiv:2304.13637*, 2023.
- [66] T. Harada, C.-M. Yoo, and K. Kohri, “Threshold of primordial black hole formation,” *Phys. Rev. D*, vol. 88, p. 084051, 2013. DOI: 10.1103/PhysRevD.88.084051. arXiv: 1309.4201 [astro-ph.CO].